



Published in final edited form as:

Soft Matter. 2013 December 21; 9(47): . doi:10.1039/C3SM52250D.

PAMAM Dendrimers as Quantized Building Blocks for Novel Nanostructures

Mallory A. van Dongen^{1,3}, S. Vaidyanathan^{3,4}, and Mark M. Banaszak Holl^{1,2,3,4,*}

¹Department of Chemistry, University of Michigan, Ann Arbor, MI 48109, USA

²Macromolecular Science and Engineering, University of Michigan, Ann Arbor, MI 48109, USA

³Department of Biomedical Engineering, University of Michigan, Ann Arbor, MI 48109, USA

⁴Michigan Nanotechnology Institute for Medicine and Biological Sciences, University of Michigan, Ann Arbor, MI 48109, USA

Abstract

The desire to synthesize soft supramolecular structures with size scales similar to biological systems has led to work in assembly of polymeric nanomaterials. Recent advances in the isolation of generationally homogenous poly(amidoamine) (PAMAM) dendrimer enables their use as quantized building blocks. Here, we report their assembly into precise nanoclusters. In this work, click-functional ligands are stochastically conjugated to monomeric generation 5 PAMAM dendrimer and separated via reverse-phase HPLC to isolate dendrimers with precise numbers of click ligands per dendrimer particle. The click-ligand/dendrimer conjugates are then employed as modular building blocks for the synthesis of defined nanostructures. Complimentary click chemistry employing dendrimers with 1, 2, 3, or 4 ring-strained cyclooctyne ligands and dendrimers with 1 azide ligand were utilized to prepare megamer structures containing 2 to 5 ~30,000 kDa monomer units as characterized by mass spectrometry, size exclusion chromatography, and reverse-phase liquid chromatography. The resulting structures are flexible with masses ranging from 60,000 to 150,000 kDa, and are soluble in water, methanol, and dimethylsulfoxide.

Keywords

Nano-periodicity; PAMAM dendrimer; Megamer; Click chemistry; Supramolecular architectures

Introduction

The need to address biological challenges across multiple hierarchical levels ranging from molecules to cells to tissue has increased the demand for synthetic strategies leading to well-defined structures on a nanometer to micron scale. Achieving such size ranges with classic synthetic strategies remains challenging. Tomalia proposed the utilization of dendrimers as quantized building blocks, termed “soft super atoms”, combined with controlled assembly to substantially expand the range of size scales available for soft synthetic materials with controlled morphology and other physical properties.¹⁻⁴ Glotzer and Solomon have discussed an analogous proposal for the use of nanocrystals and colloidal particles as “hard super atoms”.⁵ To function as super atoms, it is necessary to have control over size, shape, and surface chemistry (i.e. reactivity) to create materials with nano-periodic trends independent of variations in the monomeric material. The assembly of synthetic

*To whom correspondence should be addressed: Phone: (734) 763-2283; mbanasza@umich.edu.

nanomaterials or super atoms generates larger nano to microscale structures that fall into the following classes: I) Extended Nanostructures, which extend infinitely in one, two or three dimensions, a class that includes fibers, sheets, and lattices II) Stochastic Nanoclusters and III) Precise Nanoclusters (Figure 1). Extended Nanostructures have precise control of local architecture in one, two, or three dimensions and stochastic sizes. Stochastic Nanoclusters have control of particle size with heterogeneity in terms of numbers of super atoms per particle. Precise Nanoclusters have monodisperse assemblies of super atoms, allowing for a digital control of nanocluster size and properties. Substantial progress has been made in the assembly of hard super atoms for all three classes employing rigid polymers,^{6, 7} gold,⁸⁻¹³ and other particles.¹⁴ Substantial efforts have also been made in the area of soft super atoms, despite the challenges associated with polydispersity of polymeric building blocks. It is the use of polymers as soft super atoms, which offer tunable surface qualities such as charge and conjugation chemistry that can enhance solubility, biological compatibility, and allow for modification with drugs, dyes, and targeting agents of interest,¹⁵ that are the focus of this report.

The dendritic polymer architecture has the potential to provide a well-defined and highly functionalizable structure for utilization as a soft super atom, building block. Assemblies utilizing dendrimers as the monomer units result in larger polymer-like structures or megamers.^{16, 17} Work in this field has been pioneered by Tomalia¹⁸⁻²¹ with the “tecto-dendrimer” strategy of self-assembling shell dendrimers around a core dendrimer followed by covalent cross-linking. This class of nanostructures utilizes steric hindrance to saturate the core dendrimer with various sized (i.e. generation) shell dendrimers to create megamers resulting in precise nanostructures. Surface modification, with reactions such as acetylation, allows for fewer shell dendrimers to saturate the surface to give modular control of the resulting structures, but relying on stochastic reactions leads to a loss of precisely controlled structures.²⁹ Tecto-dendrimer assembly allows for building large megamers without encountering limiting generation effects³⁰ such as loss of flexibility, low solubility, and increased polydispersity of monomeric dendrimers of similar size ranges.¹⁸ The self-assembly approach has been shown to yield structures of Class II with a fairly narrow mass and size range but does not allow systematic, modular variation of the number of components.

An alternative approach has been to use cross-linkers to assemble groups of small dendrimers or dendrons into hierarchical structures. Such techniques have been successfully employed to synthesize extended supramolecular structures such as Class I porous networks^{17, 31, 32}, one dimensional structures³³, and two and three dimension structures (exemplified by Percec et al.).^{34, 35} There are also examples of the assembly of dendrimers into Class II supramolecular nanoparticles with modular size control via crosslinking with linear polymers.²⁵

Class III precise, three-dimensional architectures have been synthesized using chemistries to specifically link controlled numbers of dendrons together through the focal point²⁶ or through single ligands on two dendrimers.^{22, 28} The former approach, while resulting in precise nanoclusters, is limited by control over functionality of both the linking system and the dendron. To date, only small (4,000 to 30,000 Da) precise dendron-based dumbbell nanostructures have been assembled.^{26, 36} A particularly interesting example by Liu et al. assembled dendrons around a streptavidin to form tetramer-like clusters, an approach limited by the number of binding sites on the protein linker system.²⁷ Table 1 gives a summary of the synthesis strategy and characterization of previous soft super atom Class II and III materials.

Poly(amidoamine) (PAMAM) dendrimers are of particular interest for implementation as soft super atoms due to their advantageous properties such as aqueous solubility, biocompatibility, and functionalizable surface groups. The dendrimers implemented in this work are fifth generation synthesized divergently from an ethylenediamine core.³⁷ In this work, the positively charged primary amine surface has been neutralized via acetylation, which decreases the cytotoxicity of the material and increases resolution of the species in the reverse-phase high performance liquid chromatography (rp-HPLC) methods employed. Although previous studies indicated the potential of dendrimers to serve as soft super atoms, synthetic by-products in PAMAM dendrimer lead to trailing generation and oligomeric impurities ranging from 1.4 to 115 kDa. The presence of these impurity species represent an important limitation on the degree of homogeneity one can hope to achieve for the self-assembled or linked megamer products and represent an important difference between this class of super atoms and the actual atoms they are meant to mimic.

Recent work by van Dongen, Banaszak Holl et. al has enabled the isolation of monomeric PAMAM dendrimer for use as a soft super atom.³⁸ Here, we implement a method to synthesize assemblies of monomeric dendrimers via click chemistry. Our approach differs from previous strategies in the following ways: 1) our soft super atom, G5 PAMAM, does not contain the trailing generations, dimer, and trimer that typically remain in G5 and higher generation PAMAM preparations^{38, 39} 2) we assemble dendrimers containing defined numbers of ligands per dendrimer particle, 3) a digital set of precise, flexible structures has been generated ranging from 30 to 150 kDa using ~30 kDa units. This strategy differs from previous approaches that relied on self-assembly determined by dendrimer size or employed dendrimers containing a stochastic distribution of ligands per dendrimer or polymer particle.

Materials

All chemicals and materials were purchased from Sigma Aldrich or Fischer Scientific and used as received unless otherwise specified. Monomer G5 PAMAM dendrimer was purchased from Dendritech and purified as previously reported to remove trailing and oligomer impurities.³⁸ Click-Easy™ MFCO-N-hydroxysuccinimide was purchased from Berry & Associates Synthetic Medicinal Chemistry. 3-(4-(2-azidoethoxy)phenyl)propanoic acid (azide ligand) was prepared as described previously.⁴⁰

Preparation of G5-Ac-MFCO_{4.0(avg)} and G5-Ac-Azide_{4.0(avg)} conjugates

Conjugates were prepared using monomer G5, and azide ligand or Click-Easy™ MFCO-N-hydroxysuccinimide. Amine-terminated G5 (319.6 mg for azide conjugate, 299.5 mg for MFCO conjugate) was dissolved to give a 0.16 μM solution in deionized water (DI). The azide ligand (10 mg) was pre-activated in a solution at 22 mM in acetonitrile (2.5 mL) with 58 mM 1-ethyl-3-(3-dimethylaminopropyl)carbodiimide (24.1 mg) and 60 mM N-hydroxysuccinimide (14.4 mg). Click-Easy™ MFCO-N-hydroxysuccinimide (9.3 mg) was not pre-activated and was prepared by dissolving to 10.5 μM in acetonitrile (2.3 mL). Four molar equivalents of the ligand solution was added dropwise via syringe pump to the dendrimer solutions. The solutions were stirred overnight. The products were purified using Amicon Ultra Centrifugal units, 10kDa cutoff membranes, 2 PBS washes and 4 DI washes. A white solid was isolated via lyophilization for each conjugate (204.7 mg for azide conjugate, 231.1 mg for MFCO conjugate). The materials were then fully acetylated by redissolving in anhydrous methanol (0.19 μM, 30 mL) and adding 450 equiv of triethylamine and 360 equiv of acetic anhydride, stirring for 4 hours, the methanol was then removed and the sample redissolved in water, purified by the same centrifugation protocols previously described, and isolated by lyophilization. G5-Ac-MFCO_{4.0(avg)} and G5-Ac-Azide_{4.0(avg)} were characterized by rp-UPLC and ¹H-NMR (see supporting information).

Isolation of conjugates containing precisely defined ratios of G5-Ac-MFCO_n (n = 1 – 4) and G5-Ac-Azide_n (n = 1 – 4)

Dendrimers containing precise ratios of MFCO or azide ligands per particle were isolated via rp-HPLC. Multiple injections of G5-Ac-MFCO_{4.0(avg)} or G5-Ac-Azide_{4.0(avg)} were performed on a C18 column using a water/acetonitrile gradient with 0.1% TFA. Fractions were collected as the material eluted and combined to obtain samples with ratios of n = 0, 1, 2, 3, and 4 MFCO or azide ligands, and a final sample that contained dendrimer with 4 or more click ligands. Products were purified using PD-10 desalting protocols as specified in the instruction manual, with DI used as the equilibration buffer and samples initially dissolved in 10xPBS, then lyophilized to dry. Samples were characterized by rp-UPLC and ¹H-NMR. Curve fitting of UPLCs using Igor Pro was performed to provide yield, purity, and rp-HPLC number of MFCO averages (see supporting information).

Synthesis of megamer samples

n (n = 1 – 4) equivalents of G5-Ac-Azide₁ was dissolved to give a 300 μM solution in dimethylsulfoxide. To this, 1 equivalent of G5-Ac-MFCO_n (n = 1 – 4) was added. For example, to prepare the tetramer sample (n = 3), 2.7 mg of G5-Ac-Azide₁ was dissolved in 273 μL of DMSO, then 0.9 mg of G5-Ac-MFCO₃ was added. Solutions were protected from light and agitated for 48 hours. The samples were lyophilized to give white solids.

Methods

High Performance Liquid Chromatography

Isolation of G5-Ac-MFCO_n (n = 1 – 4) and G5-Ac-Azide_n (n = 1 – 4) fractions was achieved using a Phenomenex Jupiter 3003 C18 Prep Column (21.2 × 150 mm, 5 μm particles) equipped with a Waters 600 Controller, Waters 2707 Autosampler, and Waters 2998 Photodiode Array running Empower 2 Software, additionally equipped with a Waters Fraction Collector III. The weak solvent (Solvent A) was HPLC Grade Water with 0.1% TFA, and the strong solvent (Solvent B) was HPLC Grade Acetonitrile with 0.1% TFA. The gradient employed was as follows: 2.1 min load step at 95%A/5%B, 3.9 min gradient to 80%A/20%B, 15 min gradient to 65%A/35%B, 5 min gradient to 55%A/45%B, followed by 3 min was at 20%A/80%B, then equilibrating at starting conditions for 5 min before next injection. G5-Ac-MFCO_{4.0(avg)} or G5-Ac-Azide_{4.0(avg)} was dissolved to 20 mg/mL concentration and 910 uL injections were used. Five second fractions were collected starting at 9 min 30 sec into each run for a total of 120 fractions. rp-UPLCs were performed with a scaled method using an Agilent 2.1 × 100 mm column.

LC Peak Fitting

rp-UPLC chromatograms were fit with Gaussian peaks using Igor Pro Version 6.0.3.1 software. Peak widths within a chromatogram were kept constant.

Nuclear Magnetic Resonance Spectroscopy

NMR experiments were performed on Varian VNMRs 500. ¹H-NMR spectra were obtained used 10 second pre-acquisition delays and a total of 64 scans. All sample solutions were set to an approximate dendrimer concentration of 5 mg/mL in deuterium oxide.

Gel Permeation Chromatography

Gel permeation chromatography experiments were performed on an Alliance Waters 2695 separation module equipped with a 2487 dual wavelength UV absorbance detector (Waters Corporation), a Wyatt HELEOS Multi Angle Laser Light Scattering (MALLS) detector, and an Optilab rEX differential refractometer. Columns employed were Tosoh TSK-Gel

Guard PHW 06762 (75 mm × 7.5 mm, 12 mm), G 2000 PW 05761 (300 mm × 7.5 mm, 10 mm), G 3000 PW 05762 (300 mm × 7.5 mm, 10 mm), and G 4000 PW (300 mm × 7.5 mm, 1 mm). Column temperature was maintained at 25 ± 0.1 °C with a Waters temperature control module. The isocratic mobile phase was 0.1 M citric acid and 0.025 wt % sodium azide, pH 2.74, at a flow rate of 1 mL/min. The sample concentration was 10 mg/5 mL with an injection volume of 100 μ L. This was used to calculate the weight average molecular weight, M_w , and the number average molecular weight, M_n , with Astra 5.3.2 software. Values for dn/dc were kept at a constant of 0.215.

Mass Spectrometry

Matrix-assisted Laser-Desorption Time-of-Flight Mass Spectrometry (MALDI-TOF-MS) was performed using a MALDI Micro MX running MassLynx Version 4.0 software. Dendrimer samples were prepared by dissolving in DI water at concentration 10 mg/mL, then serial diluting with methanol 1:1, then 1:4. The samples were then mixed 1:1 with the matrix dihydroxybenzoic acid (concentration of 10 mg/mL in 1:1 water/acetonitrile) and spotted on to a MALDI plate. Samples were calibrated using bovine serum albumin with a matrix of sinapic acid. At least 150 laser shots were compiled for each spectrum. The spectra were smoothed using the MassLynx Software settings of Smooth window (channels) equals 12, and Number of smooths equals 12. No baseline subtraction or peak centering was performed.

Results and Discussion

PAMAM dendrimers have been extensively studied as nanoscale biomedical devices due to their low polydispersity, multiple sites for chemical modification, flexibility, water solubility at high generations, and biocompatibility.^{15, 41, 42} Recent work has employed rp-HPLC to remove both generational and oligomer (primarily dimer and trimer) impurities from generation 5 (G5) PAMAM to obtain samples of G5 monomer with a PDI under 1.02 (Figure 2).³⁸ The mass dispersity of the building block materials has been reduced from greater than 100 kDa to less than 3 kDa. In order to assemble these monomeric units into controlled megamer units, we have employed our methods for attaching precise numbers of click conjugation functional groups per dendrimer particle.^{40, 43, 44} This synthetic strategy generates materials with precise ligand/particle ratios in a manner that is independent of the mass dispersity of the soft super atom scaffold, thus decoupling mass dispersity and particle assembly. Although work in the tecto-dendrimer field has been successful in generating highly homogenous assemblies of dendrimers, the size of these clusters is pre-determined by the size of the core and shell dendrimers and cannot be modularly controlled. For example, assembly of G5 PAMAM around a core G7 PAMAM yielded primarily G7(G5)₁₂, with incompletely packed shells containing 9 to 11 G5 per G7 also observed.²⁰ The self-assembly process does not allow for the generation of a controlled set of samples to stoichiometry G7(G5)_n where n is digitally varied. In addition, dispersity in numbers of G5 packing around G7 may arise from the molecular weight distribution present in both the G5 and G7 samples including trailing generations and oligomers.

The synthetic strategy for the click conjugates and megamers is outlined in Scheme 1. First, a stochastic conjugation via a peptide bond to an azide or ring-strained cyclooctyne click ligand is followed by acetylation of all remaining primary amine groups. These materials are designated G5-Ac-MFCO_{n(avg)} and G5-Ac-Azide_{n(avg)}. In order to optimize the amount of material for isolation of dendrimer containing 1–4 click linkers, an initial stochastic average of 3–4 ligands/particle was typically employed. Isolation of dendrimer samples containing precise click-ligand/dendrimer ratios, as opposed to an average ratio made of up a Poisson distribution, was achieved using semi-preparative scale rp-HPLC (Figure 3a) following previously published protocols.^{40, 43} The dendrimers are retained on the hydrophobic C18

column as a function of the number (n) of hydrophobic ligands conjugated to the dendrimer surface. This model is supported by the increased resolution of the MFCO conjugate, which contains the hydrophobic cyclooctyne entity and a 5 carbon linker, as compared to the azide conjugate. The successful application of this isolation process to the commercially available MFCO ligand demonstrates a broader versatility for this separation process. rp-UPLC was employed to confirm that successful separation was achieved (Figures 3b, S1). The initial stochastic distribution of click ligand on the dendrimer can be visualized⁴⁵ and subsequently separated via rp-HPLC due to increased retention time with the increasing numbers of hydrophobic ligands available for interaction with the hydrophobic C18 stationary phase.^{40, 43, 44} These materials are designated G5-Ac-MFCO _{n} ($n = 1 - 4$) and G5-Ac-Azide _{n} ($n = 1 - 4$). ¹H NMR also confirmed that the desired click-ligand/dendrimer ratios had been achieved (Figures S2, S3; Tables S1, S2). In assessing the purity of each isolated fraction containing the precisely defined ligand/particle ratio (n ligands per dendrimer), rp-UPLC provides the most direct measure. The separation is based on the number of hydrophobic ligands per particle and excellent separation is achieved. The G5 PAMAM dendrimers are flexible enough to effectively display the ligands to the hydrophobic C18 support regardless of their relative conjugation point on the PAMAM scaffold. The assessment of the ligand/particle ratio by ¹H NMR requires a number of key assumptions and relies on average polymer properties at key points of the analysis. The NMR-based ratio is determined by comparing the integration of the ligand protons to the integration of the terminal –NHC(O)CH₃ groups on the dendrimer. This analysis suffers from comparing a small value (the ligand) to a large value (acetamide group) and from having to employ an average number of these groups for G5 PAMAM of 93, although this number varies from ~70 to 116 for each particle. For these reasons, we believe the rp-UPLC measurement provides the better quantitative analysis of ligand/particle ratio.

Peak fitting of rp-UPLC also allows for an estimation of the relative amount of each ligand/particle ratio in the initial averaged sample and in turn for an estimation of percent recovery of the precise product from the stochastic mixture (supporting information). The recovery of the components utilized in this work (G5-Ac-MFCO _{n} $n = 1 - 4$ and G5-Ac-Azide₁) range from 43% to 77%. These represent the yield of the final clicked megamer products as well since complete recovery of samples is possible without further purification.

Through combination of precise ratio ligand-to-dendrimer G5 monomers containing $n = 1$ azide ligand and $n = 1 - 4$ cyclooctyne ligands, we have synthesized a digital set of modular and precise megamer nanostructures (Scheme 2, Figures 4 and 5). G5 dimers, trimers, tetramers (one core with three shell dendrimers), and pentamers (one core with four shell dendrimers) have been synthesized from a click reaction between G5 with 1 azide ligand to G5 conjugated to 1, 2, 3, and 4 monofluorinated cyclooctyne (MFCO) ligands, respectively. Briefly, G5-Ac-Azide₁ was added in equimolar, two-fold, three-fold, or four-fold equivalents to 1–2 mg G5-Ac-MFCO _{n} ($n = 1 - 4$), respectively and mixed for 48 hours. The product peaks illustrated in Figure 4 (orange for dimer, green for trimer, blue for tetramer, purple for pentamer, color designations that will be kept for the remainder of this article) are shifted to the left with respect to the G5-Ac-Azide₁ starting material (yellow) and G5-Ac-MFCO _{n} ($n = 1 - 4$) starting material (pink), indicating less interaction with the hydrophobic column after formation of the click linkage. Solid samples were isolated for G5-(G5) _{n} ($n = 1 - 4$) megamers by lyophilization. For $n = 1$ and 2, each reactant peak was entirely consumed. For $n = 3$ and 4, smaller peaks (*) are present in addition to the desired product peak that are most likely unreacted G5-Azide₁ although partially reacted G5-Ac-MFCO_{4- n} -G5-Ac-Azide _{n} cannot be ruled out. Small peaks for partially reacted G5-G5 _{m} -MFCO _{$n-m$} species also appear for the trimer, tetramer, and pentamer samples (#), which may result from cyclooctyne ligands becoming sterically blocked by previously clicked dendrimers on the particle or by small errors in the stoichiometry of addition. Other possible assignments

for the * and # peaks include regioisomers of the location of the clicked dendrimers on the central dendrimer surface as well as structural isomers resulting from the two possible click isomers. We do not favor these last two hypotheses since we do not anticipate this large of a shift (click regioisomers) and believe a broad distribution of products (resulting from surface regioisomers) is unlikely to result in the discrete peaks observed. Possible side products resulting from incomplete reaction and the regiochemistry of the click reaction are schematically depicted in Figure S4. The purity of the isolated materials as illustrated in Figure 4 can be compared to anticipated distribution of products if stochastic averages of G5-Ac-Azide₁ and G5-Ac-MFCO_n (n = 1 – 4) had been employed. Combining the stochastically prepared materials for cycloalkyne n_{avg} 1 – 4 and azide n_{avg} = 1 would yield mixtures containing roughly 16, 24, 28, and 36 primary products.^{43, 44}

In order to help visualize the structures, scale models are illustrated in Figure 5. The top row, with dendrimer units spaced apart, emphasizes the connectivity, although it is important to note that for all megamer samples the dendrimers on the periphery are bound to a distribution of the flexible surface arm locations. The bottom row, with dendrimer units in van der Waals contact, is likely the more realistic view of megamer structure in aqueous solvent based on previous computational work.⁴⁶

MALDI-TOF-MS (Figure 6) was consistent with the rp-UPLC structure assignments. A mass increase of approximately 30 kDa, corresponding to expected molecular weight change from the monomer (red), to the dimer (orange), trimer (green), tetramer (blue), and pentamer (purple) is observed. In the pentamer, the [M₅]⁺ peak can be readily seen at approximately 150 kDa, which is not present in the monomer sample. Additionally, a distinct 75 kDa peak corresponds to [M₅]²⁺. Similarly, the [M₃]⁺ peak is present for the trimer at 90 kDa with a [M₃]²⁺ peak evident at 45 kDa. A peak for the parent ion of [M₄]⁺ appears at 120 kDa along with a peak at the expected mass of 60 kDa for [M₄]²⁺; however, in this case an interfering peak precludes an unambiguous assignment for the doubly ionized species. Similarly, a peak is apparent at 60 kDa for dimer [M₂]⁺ although the monomer also gives some signal at this position, albeit at a substantially reduced intensity. These data are consistent with the formation of the controlled ratio materials; however, similar to the NMR analysis it is complicated by the dispersity of the monomer G5 scaffold, which has mass distribution ranging from roughly 22,000 to 27,000 kDa.³⁸

The samples were further characterized by gel permeation chromatography (GPC). The cumulative data function shows steps of approximately 30 kDa, corresponding molecular weight of the acetylated G5 monomer (Figure 7a). Increased heterogeneity, as demonstrated by deviation of the megamer slopes from vertical, arising from additive branching-type structural defects that are still present in the G5 monomer starting material, is both expected and observed as number of monomer units increases from 1 (red, monomer) to 5 (purple, pentamer).

This can be further demonstrated by dividing each megamer structure by the number of monomer units it contains (e.g. dimer by 2, trimer by 3, see Figure 7b) where the resulting plots have similar slopes. In this instance, the presence of the mass dispersity actually provides additional support for the assigned structures. Steps in the larger megamers are also seen, corresponding to small amounts of incompletely reacted materials still present in the sample. Table 2 summarizes the GPC molecular weight results. The average molecular weight changes in multiples of the monomer mass. The less-than-ideal ratio for the pentamer is consistent the presence of unreacted partial click reaction as observed by UPLC.

The removal of oligomeric defects that constituted over 20% by mass of commercial PAMAM material has enabled the synthesis of these megamer structures with low

polydispersity. As demonstrated in previous work from this group³⁸, the rp-HPLC methods employed here to isolate dendrimers as a function of number of hydrophobic ligands also separate oligomer defects within the G5 PAMAM. As a result, oligomers conjugated to n-1 ligands co-elute with monomers conjugated to n ligands (for example, Dimeric G5-MFCO₁ co-elutes with Monomeric-MFCO₂). Such impurities in the starting material would create side products in megamer assembly with molecular weights double the theoretical value and greatly increase the polydispersity. The successful removal of the oligomeric side products reduces the high molecular weight impurities as measured by GPC in Figure 7a.

Conclusions

This work, demonstrating the use of PAMAM dendrimers containing precisely defined ligand/particle ratios as building blocks for generating controlled nanostructures in the 30 to 150 kDa size range, advances the use of dendrimers as quantized building blocks for homogenous megamers the size of large proteins and multi protein constructs. The HPLC isolation platform has proven to be efficient and versatile,^{40, 43} with similar preparation and isolation procedures for at least 4 complimentary click ligands to date allowing for diverse chemistries to be utilized with high (30%–80%) recovery of precise ligand/particle materials from the stochastic mixture. The one-pot self-assembly creates stable, covalently bound megamers that are soluble in water and organic solvents methanol and dimethylsulfoxide, making them promising candidates for both biological environments and functionalization.

Supplementary Material

Refer to Web version on PubMed Central for supplementary material.

Acknowledgments

The authors thank C. A. Dougherty for fruitful discussions, D. G. Mullen for ligand synthesis, and Brian Shay of the Biomedical Mass Spectrometry Facility for MALDI assistance. This project has been funded in part with Federal funds from the National Institutes of Health, National Institute of Biomedical Imaging and Bioengineering under Award EB005028.

References

1. Tomalia DA. *Soft Matter*. 2010; 6:456–474.
2. Tomalia DA. *J Nanopart Res*. 2009; 11:1251–1310. [PubMed: 21170133]
3. Tomalia, DA.; Christensen, JB.; Boas, U. *Dendrimers, Dendrons and Dendritic Polymers: Discovery, Applications, the Future*. Cambridge University Press; NY: 2012. p. 293-377.
4. Christensen, JB.; Tomalia, DA. *Dendrimers as Quantized Nano-modules in the Nanotechnology Field*. Campagna, S.; Ceroni, P.; Puntoriero, F., editors. J. Wiley & Sons; Hoboken: 2012. p. 1-33.
5. Glotzer SC, Solomon MJ. *Nature Materials*. 2007; 6:557–562.
6. Chen Q, Whitmer JK, Jiang S, Bae SC, Luijten E, Granick S. *Science*. 2011; 331:199–202. [PubMed: 21233384]
7. Wang YF, Wang Y, Breed DR, Manoharan VN, Feng L, Hollingsworth AD, Weck M, Pine DJ. *Nature*. 2012; 491:51–U61. [PubMed: 23128225]
8. Mirkin CA, Letsinger RL, Mucic RC, Storhoff JJ. *Nature*. 1996; 382:607–609. [PubMed: 8757129]
9. Alivisatos AP, Johnsson KP, Peng XG, Wilson TE, Loweth CJ, Bruchez MP, Schultz PG. *Nature*. 1996; 382:609–611. [PubMed: 8757130]
10. Feng L, Dreyfus R, Sha RJ, Seeman NC, Chaikin PM. *Adv Mater*. 2013; 25:2779–2783. [PubMed: 23554152]
11. Ofir Y, Samanta B, Rotello VM. *Chem Soc Rev*. 2008; 37:1814–1823. [PubMed: 18762831]
12. Zhang C, Macfarlane RJ, Young KL, Choi CHJ, Hao L, Auyeung E, Lui G, Zhou X, Mirkin CA. *Nature Mat*. 2013; 12:741–746.

13. Larson-Smith K, Pozzo DC. *Soft Matter*. 2011; 7:5339–5347.
14. Tang ZY, Zhang ZL, Wang Y, Glotzer SC, Kotov NA. *Science*. 2006; 314:274–278. [PubMed: 17038616]
15. Svenson S. *Eur J Pharm Biopharm*. 2009; 71:445–462. [PubMed: 18976707]
16. Khopade AJ, Mohwald H. *Macromol Rapid Comm*. 2005; 26:445–449.
17. Kiran BM, Jayaraman N. *Macromolecules*. 2009; 42:7353–7359.
18. Tomalia DA. *Prog in Polymer Sci*. 2005; 30:294–324.
19. Uppuluri S, Keinath SE, Tomalia DA, Dvornic PR. *Macromolecules*. 1998; 31:4498–4510.
20. Betley TA, Hessler JA, Mecke A, Banaszak Holl MM, Orr BG, Uppuluri S, Tomalia DA, Baker JR Jr. *Langmuir*. 2002; 18:3127–3133.
21. Li J, Swanson DR, Qin D, Brothers HM, Piehler LT, Tomalia DA, Meier DJ. *Langmuir*. 1999; 15:7347–7350.
22. Mullen DG, McNerny DQ, Desai A, Cheng X-m, DiMaggio SC, Kotlyar A, Zhong Y, Qin S, Kelly CV, Thomas T, Majoros IJ, Orr BG, Baker JR Jr, Banaszak Holl MM. *Bioconjugate Chem*. 2011; 22:679–689.
23. Uppuluri S, Swanson DR, Piehler LT, Hagnauer GL, Tomalia DA. *Adv Mater*. 2000; 12:796–800.
24. Tomalia DA, Uppuluri S, Swanson DR, Li J. *Pure Appl Chem*. 2000; 72:2343–2358.
25. Wang H, Wang S, Su H, Chen K-J, Armijo AL, Lin W-Y, Wang Y, Sun J, Kamei K-i, Czernin J, Radu CG, Tseng H-R. *Angew Chem Int Ed Engl*. 2009; 48:4344–4348. [PubMed: 19425037]
26. Sung SR, Han SC, Jin SH, Lee JW. *B Kor Chem Soc*. 2011; 32:3933–3940.
27. Chen P, Sun Y, Liu H, Xu L, Fan Q, Liu D. *Soft Matter*. 2010; 6:2143–2145.
28. DeMattei CR, Huang B, Tomalia DA. *Nano Letters*. 2004; 4:771–777.
29. Tomalia DA, HMB, Piehler LT, Durst HD, Swanson DR. *Proc Natl Acad Sci USA*. 2002; 99:5081–5087. [PubMed: 11943851]
30. de Gennes PG, Hervet H. *J Physique Lett*. 1983; 44:351–360.
31. Brahmi Y, Katir N, Hameau A, Essoumhi A, Essassi EM, Caminade A-M, Bousmina M, Majoral J-P, El Kabib A. *Chem Comm*. 2011; 47:8626–8628. [PubMed: 21717005]
32. Kozaki M, Tujimura H, Suzuki S, Okada K. *Tetrahedron Lett*. 2008; 49:2931–2934.
33. Garzoni M, Cheval N, Fahmi A, Dananni A, Pavan GM. *J Am Chem Soc*. 2012; 134:3349–3357. [PubMed: 22263548]
34. Percec V, Ahn CH, Ungar G, Yeardley DJP, Moller M, Sheiko SS. *Nature*. 1998; 39:161–164.
35. Percec V, Cho WD, Mosier PE, Ungar G, Yeardley DJP. *J Am Chem Soc*. 1998; 120:11061–11070.
36. Rudzevich Y, Rudzevich V, Moon C, Brunklaus G, Bohmer V. *Org Biomol Chem*. 2008; 6:2270–2275. [PubMed: 18563259]
37. Tomalia, DA.; Christensen, JB.; Boas, U. *Dendrimers, Dendrons and Dendritic Polymers: Discovery, Applications, the Future*. Cambridge University Press; NY: 2012. p. 30
38. van Dongen MA, Desai A, Orr BG, Baker JR Jr, Banaszak Holl MM. *Polymer*. 2013; 54:4126–4133. [PubMed: 24058210]
39. Mullen DG, Desai A, van Dongen MA, Barash M, Baker JR Jr, Banaszak Holl MM. *Macromolecules*. 2012; 45:5316–5320. [PubMed: 23180887]
40. Mullen DM, Borgmeier EL, Desai A, van Dongen MA, Barash M, Chen X-M, Baker JR Jr, Orr BG, Banaszak Holl MM. *Chem Eur J*. 2010; 10:10675–10678. [PubMed: 20683917]
41. Pettit MW, Griffiths P, Ferruti P, Richardson SC. *Therapeutic Delivery*. 2011; 2:907–917. [PubMed: 22833902]
42. Tomalia DA, Reyna LA, Svenson S. *Biochem Soc Trans*. 2007; 35:62–67.
43. Mullen DM, Banaszak Holl MM. *Acc Chem Res*. 2011; 44:1135–1252. [PubMed: 21812474]
44. Mullen DG, Fang M, Desai A, Baker JR Jr, Orr BG, Banaszak Holl MM. *ACS Nano*. 2010; 4:657–670. [PubMed: 20131876]
45. Fréchet JMJ, Lochman L, Smigol V, Svec F. *J Chromatogr A*. 1994; 667:284–289. [PubMed: 8025631]

46. Kelly CV, Leroueil PR, Nett EK, Wereszczynski JM, Baker JR Jr, Orr BG, Banaszak Holl MM. J Phys Chem B. 2008; 112:9339–9345.

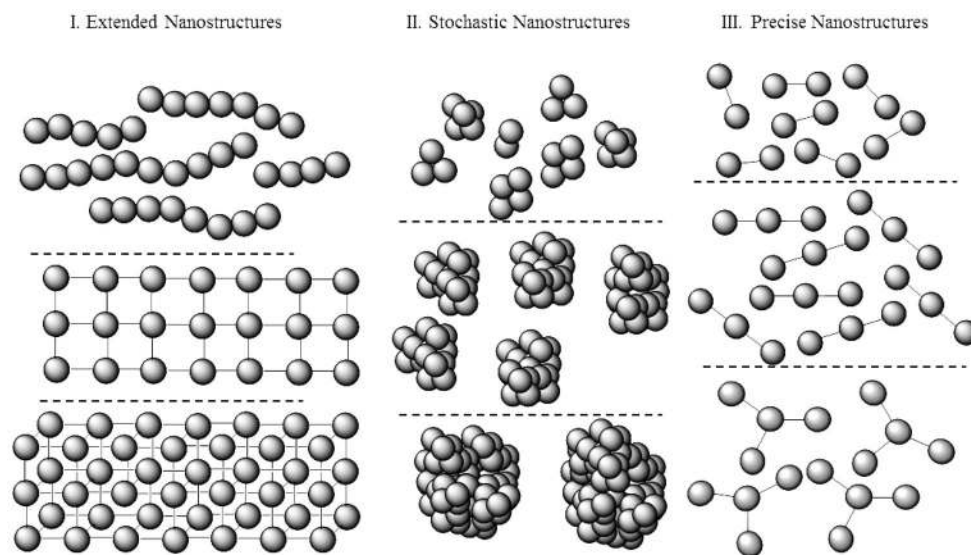


Figure 1. Controlled super atom-based nanostructures can be classified as: I) Extended Nanostructures including in one to three dimensions (for example: fibers, sheets, and lattices) II) Stochastic Nanoclusters and III) Precise Nanoclusters.

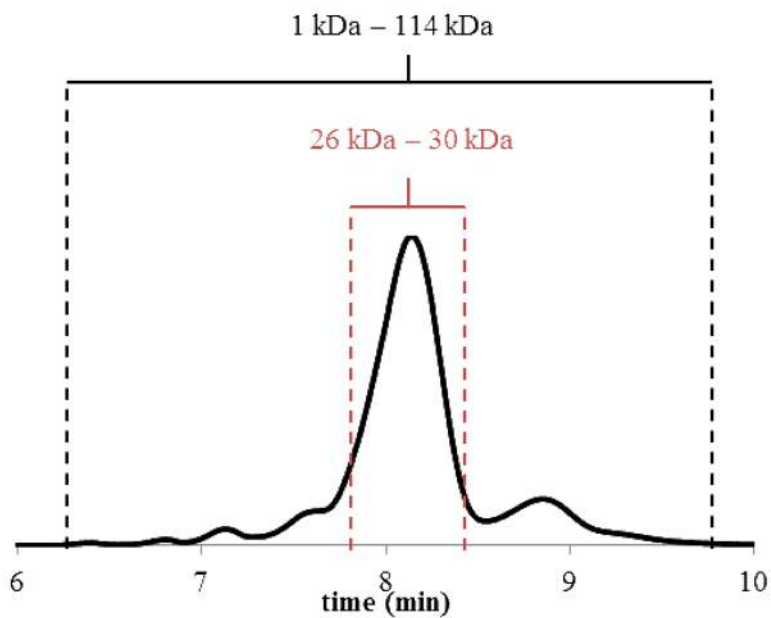


Figure 2. The monomer G5 PAMAM material used for this study is indicated by the 26 – 30 kDa fraction within the dashed red lines. Isolation of monomer G5 reduces size range of PAMAM building blocks by over an order of magnitude.

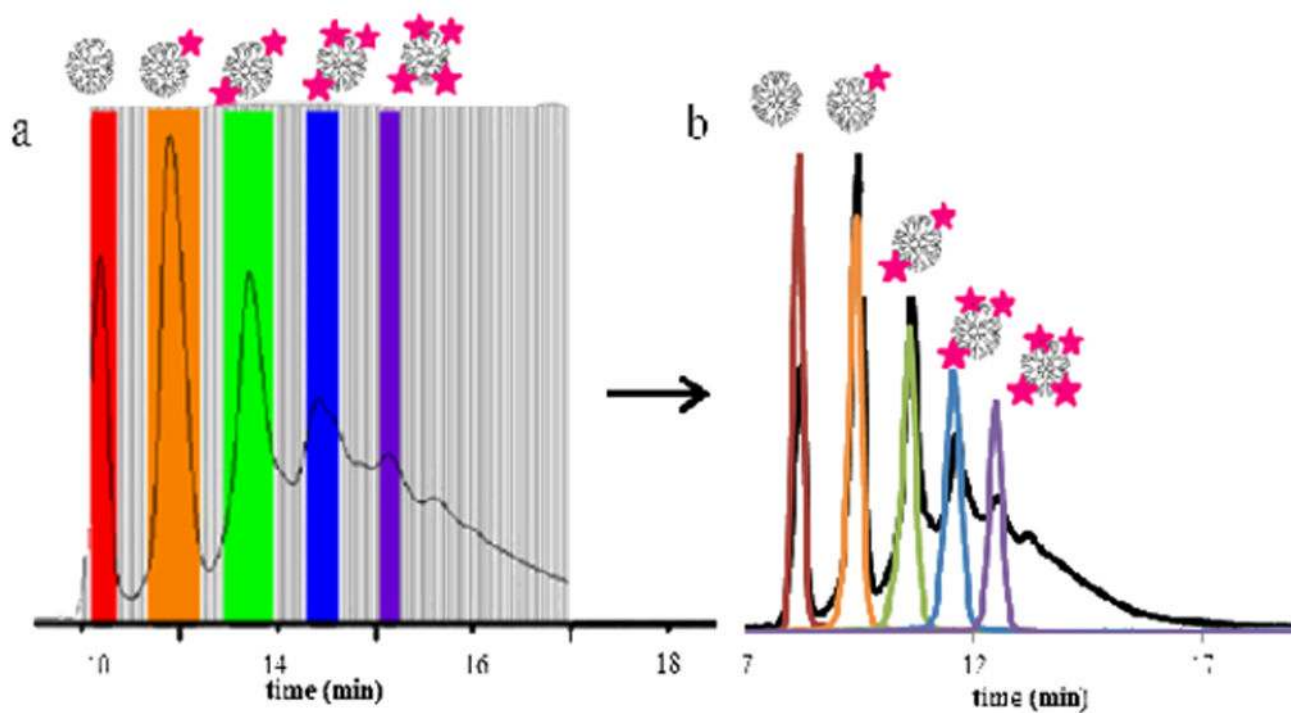


Figure 3. (a) Semi-prep rp-HPLC isolation of precisely defined G5-MFCO_n species, colored bars represent combined fractions. (b) UPLC of combined fractions demonstrates that each sample now contains a single particular ligand/dendrimer ratio.

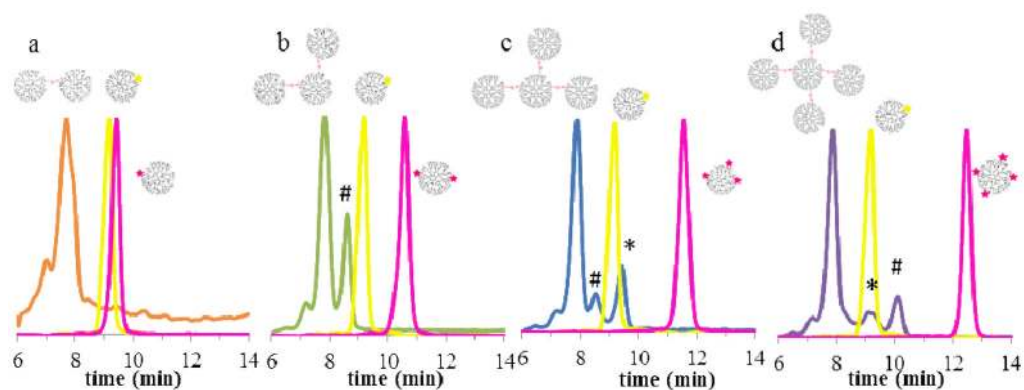


Figure 4. (a–d) UPLC chromatograms at 210 nm of dimer (a, orange), trimer (b, green), tetramer (c, blue), and pentamer (d, purple) products with the starting materials, G5-Ac-Azide₁ (cyan) and corresponding G5-Ac-MFCO_n (n= 1 – 4) (pink). The symbol “#” indicates peaks that have been assigned as incompletely clicked products and “*” indicates unreacted G5-Ac-Azide₁ in the product.

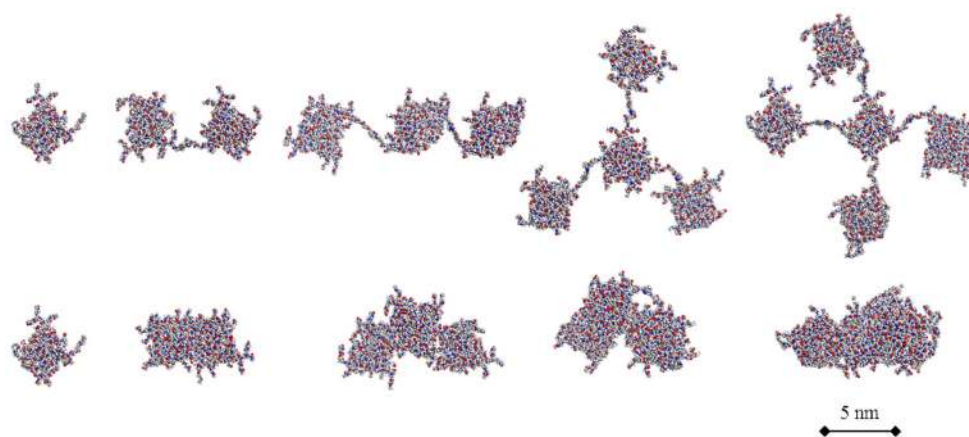


Figure 5. Scale cartoons of monomer and megamer structures generated using the COMPASS force-field in Materials Studio. The top row illustrates megamers separated by the largest distance allowed by the linker system (~ 4 nm). The bottom row depicts structures in which the dendrimers units are at a van der Waals separation distance.

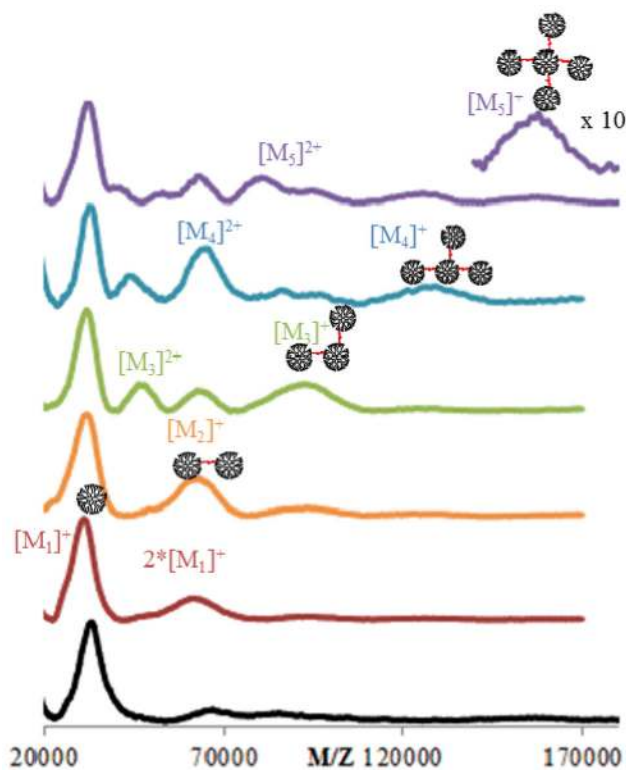


Figure 6. Normalized MALDI-TOF-MS spectra of commercial G5 PAMAM (black), G5 monomer (red), dimer (orange), trimer (green), tetramer (blue), and pentamer (purple). The $[M_5]^+$ peak has been magnified by 10 for ease of visualization.

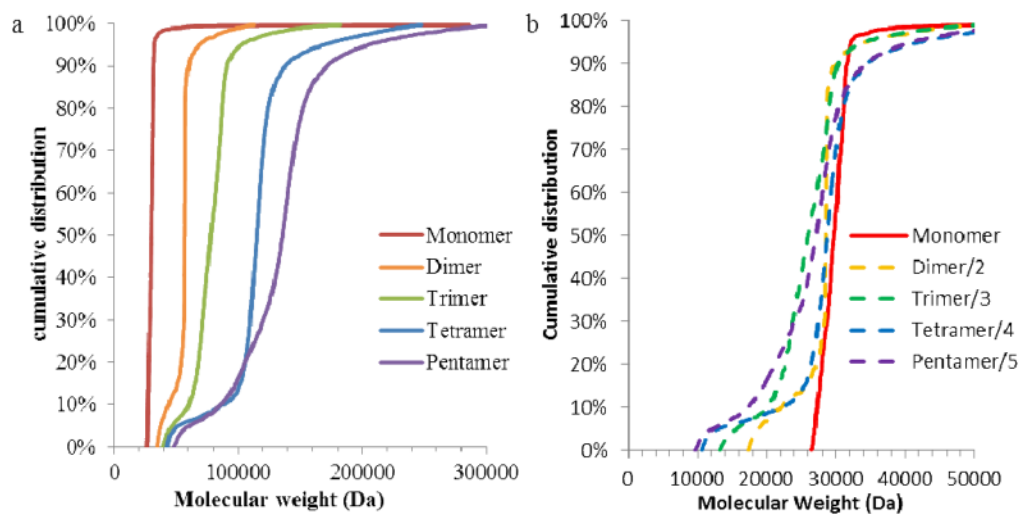
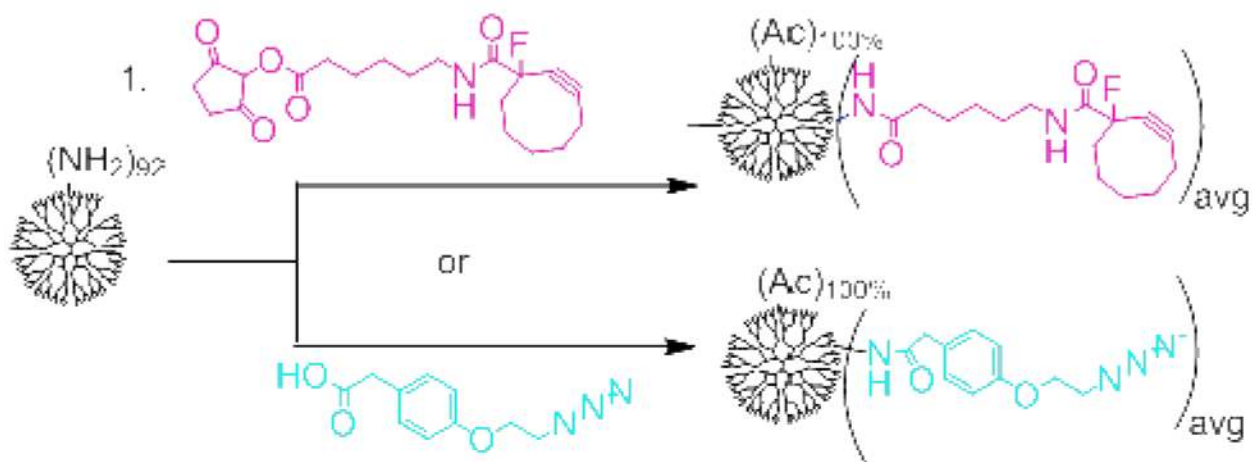


Figure 7.

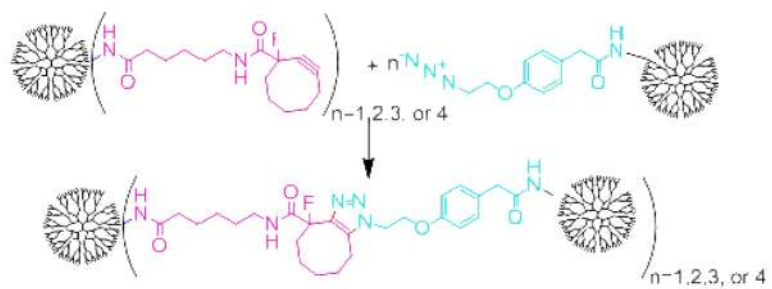
(a) Cumulative data function of M_n from GPC results. (b) Cumulative data function of each n-mer divided by n.



2. Acetic anhydride, TEA, methano

Scheme 1.

Synthesis of acetylated stochastic ligand-dendrimer conjugates.

**Scheme 2.**

Click reaction for synthesis of megamers from precisely defined dendrimer conjugates.

Table 1

Summary of soft superatom synthetic approaches and characterization.

Reference	System	Class	Mass Range	Chromatography	Mass Spec	LS	NMR	Microscopy
Present work	Dendrimer/click ligand clusters	III	30–150 kDa	GPC, rp-HPLC	MALDI	No	Proton	No
22	Dendrimer/click ligand dumbbells	II	~60 kDa	GPC	No	No	Proton	No
21, 23, 24	Tecto-dendrimers	III	300 kDa	PAGE	MALDI	No	No	AFM
25	Dendrimer/PEI clusters	II	na	No	No	Yes	No	TEM
26	PEG/dendron dumbbells	III	5 kDa	GPC	MALDI	No	Proton, Carbon	No
27	DNA/Dendron/Streptavidin	III	~100 kDa	PAGE	No	Yes	Proton	No
28	DNA/Dendron Dumbbells	III	10–30 kDa	PAGE	MALDI	No	No	No

Table 2

Quantitative summary of GPC results.

Species	Mn	Mw	PDI	Mn (megamer)/Mn (monomer)
Monomer	29,790	31,333	1.052	1.0
Dimer	57,340	59,340	1.017	1.9
Trimer	79,230	81,560	1.029	2.7
Tetramer	116,700	120,700	1.035	3.9
Pentamer	131,500	139,800	1.063	4.4